Biotechnology and Bioengineering

WILEY

BIOTECHNOLOGY AND BIOENGINEERING

ARTICLE OPEN ACCESS

Development of Peptide Glucosyltransferase Inhibitors With Comprehensive Coverage Across *Clostridioides difficile* Toxin B Sub-Types

Carly M. Catella[1] | Sudeep Sarma[1] | Caroline M. Hinesley[2] | Corey E. Febo[1] | Keith A. Breau[3] | Deniz Durmusoglu[1] | Ethan Purnell[1] | Scott T. Magness[2,3,4] | Carol K. Hall[1] | Stefano Menegatti[1,5] | Nathan Crook[1]

[1]Department of Chemical Engineering, North Carolina State University, Raleigh, North Carolina, USA | [2]Center for Gastrointestinal Biology and Disease, University of North Carolina at Chapel Hill, Chapel Hill, North Carolina, USA | [3]Department of Cell Biology and Physiology, University of North Carolina at Chapel Hill, Chapel Hill, North Carolina, USA | [4]Department of Medicine, University of North Carolina at Chapel Hill, North Carolina, USA | [5]Biomanufacturing Training and Education Center (BTEC), North Carolina State University, Raleigh, North Carolina, USA

Correspondence: Nathan Crook (nccrook@ncsu.edu)

Received: 23 July 2025 | **Revised:** 7 October 2025 | **Accepted:** 25 October 2025

Funding: National Institutes of Health; North Carolina Biotechnology Center; Novo Nordisk Fonden; National Science Foundation.

ABSTRACT

Clostridioides difficile infection presents an escalating clinical challenge due to the proliferation of hypervirulent and antibiotic-resistant strains. The primary symptoms of disease, namely colitis and diarrhea, are induced by the release of two toxins: TcdA and TcdB. Targeting these toxins with peptide inhibitors provides an attractive therapeutic strategy that can be used alone or synergistically with standard antibiotic treatments to alleviate severe symptoms and reduce the risk of resistance development. In this study, we present the rational discovery and optimization of potent TcdB peptide inhibitors. The lead sequences effectively inhibit TcdB glucosyltransferase activity, the crucial enzymatic process leading to disease symptoms, by directly competing with the toxin's molecular targets, Rho proteins. Detailed enzymatic studies also elucidate distinct Michaelis constants, K_M, for each substrate, UDP-glucose and Rho-proteins, for multiple TcdB GTD subtypes. The selected peptides demonstrated broad efficacy against the three most common TcdB subtypes, which are used in over 90% of clinical isolates. Additionally, the peptides delayed TcdB-induced loss of barrier integrity and decreased apoptosis in a primary human colon epithelial monolayer model. This study highlights a novel therapeutic avenue with significant potential to enhance the treatment and management of *C. difficile* infections.

1 | Introduction

Clostridioides difficile (*C. difficile*) is a gastrointestinal pathogen that is recognized as an urgent threat by the US Centers for Disease Control and Prevention (CDC) due to the prevalence of antibiotic resistant and hypervirulent strains causing significant morbidity, mortality, and healthcare burden (Centers for Disease Control and Prevention U.S. 2019; Rupnik et al. 2009; Schäffler and Breitrück 2018). *C. difficile* Infection (CDI) is characterized by colitis, diarrhea, inflammation, and increased epithelial permeability, which are primarily driven by the release of clostridial glucosylating toxins (Carter et al. 2015; Alonso et al. 2022; Aktories et al. 2017). Current treatment guidelines for CDI recommend discontinuing the antibiotic therapy mediating the gut dysbiosis and initiating targeted antibiotic therapy for *C. difficile* (e.g., vancomycin or fidaxomicin) (Johnson et al. 2021). However, these treatments are not always effective and may lead to recurrent infections, antibiotic

Carly M. Catella and Sudeep Sarma contributed equally to this study.

resistance, and delay the recovery of a colonization-resistant microbiome (Johnson 2009; Normington et al. 2021; Bassères et al. 2021; Spigaglia 2016; Theriot et al. 2016). Fecal microbiota transplantation (FMT) aims to facilitate the recovery of a colonization-resistant microbiome through the introduction of fecal matter or an isolated microbial consortium from healthy donors (Baunwall 2020; Khoruts et al. 2021). Two FDA approved FMT products, Rebyota (approved 2022) and Vowst (approved 2023), aim to standardize this approach (Dubberke et al. 2018; McGovern et al. 2021). While FMT is generally considered safe and effective, there are challenges in their sourcing, manufacture, and storage, and outstanding questions on treatment durability and underlying mechanism of action (Yadegar et al. 2024). Because toxin production is necessary for CDI (Lyras et al. 2009; Chandrasekaran and Lacy 2017), there has been significant interest in targeting the toxins of *C. difficile* as an orthogonal, synergistic treatment strategy to both antibiotics and microbiome restoration therapies (Durmusoglu et al. 2021; Stewart et al. 2020).

The two large clostridial glucosylating toxins (LCGTs) A and B (TcdA and TcdB), which feature 42% sequence identity and 60% similarity (Figure 1A), are the primary virulence factors of *C. difficile* (Aktories et al. 2017; Genth et al. 2014). The four domains of TcdA and TcdB enable intracellular glucosyltransferase activity: (i) the combined repetitive oligopeptides (CROPs) domain binds to cell surface receptors for internalization (Yuan et al. 2015; Ho et al. 2005); (ii) the delivery and receptor binding domain (DRBD) also mediates cell entry and translocates the toxin to the endosomal membrane upon endosomal acidification (Gerhard et al. 2013; Manse and Baldwin 2015; Tao et al. 2016; Genisyuerek et al. 2011); (iii) the cysteine protease domain (CPD), activated by inositol hexakisphosphate, releases the glucosyltransferase domain (GTD) into the cytosol (A. Shen et al. 2011); finally, (iv) the GTD inactivates Rho-family proteins through glucosylation of conserved threonine residues (Just, Wilm, et al. 1995; Just, Selzer, et al. 1995; Reinert et al. 2005) (Figure 1B). Glucosylation of these residues disrupts key signaling pathways, leading to cell rounding, disruption of the actin cytoskeleton, and degradation of tight junctions, manifesting as the hallmark pathophysiology, increased fluid secretion, mucosal permeability and damage, and release of inflammatory cytokines (Aktories et al. 2017). This inflammatory response leads to colitis and diarrhea (Aktories et al. 2017).

Decades of research have elucidated the molecular mechanisms underpinning the structure and activity of the toxins. However, to date, only one toxin inhibitor, Bezlotoxumab, has received FDA approval. Bezlotoxumab, a fully human mAb, targets two epitopes in the TcdB CROPs domain, blocking cell entry via CSPG4 receptors (Villafuerte Gálvez and Kelly 2017; Hernandez et al. 2015; P. Chen et al. 2021). A second antibody, Actoxumab, was developed against the TcdA CROPs domain, but showed no benefit alone or in combination with Bezlotoxumab and was abandoned (Hernandez et al. 2015, 2017; Raeisi et al. 2022). Several factors make inhibition of glucosyltransferase activity more attractive for drug design versus cell entry, which requires that the drug block multiple receptor binding sites across the CROPs and delivery domains (Gerhard et al. 2013; Manse and

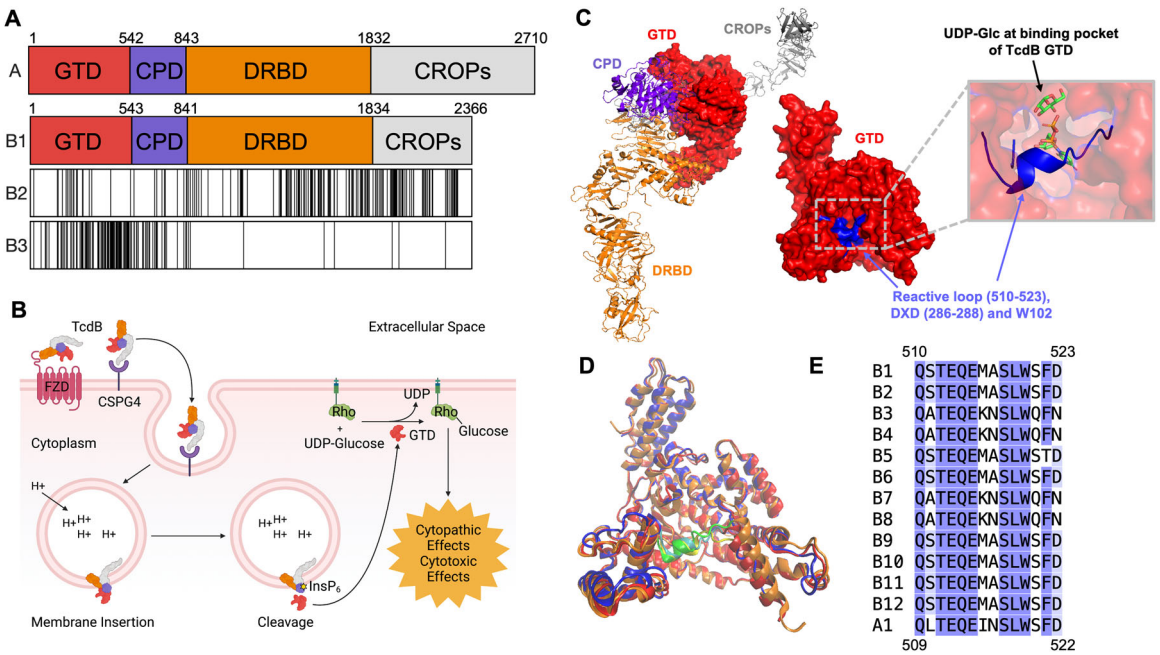

FIGURE 1 | *Clostridioides difficile* toxin structure and mechanism. (A) Sequence identity (white) of TcdB subtypes B2 (R20291) and B3 (1470) compared to B1 (VPI 10463); TcdA domain map shown for reference CPD/APD: cysteine protease (or autoproteolytic) domain; CROP: combined repetitive oligopeptides domain; DRBD: delivery and receptor binding domain; GTD: Glucosyltransferase domain. (B) TcdB mechanism: cell entry via endocytosis is mediated by receptor-binding domains in the DRBD and CROPs domain, endosomal acidification allows the DRBD to translocate across the membrane, the CPD is activated by cytosolic $InsP_6$, cleaving the GTD, which glucosylates Rho proteins. (C) Structure of TcdB holotoxin (PDB: 6OQ5), GTD (red), CPD (purple), DRBD (orange), CROPs (gray). Inset: TcdB GTD (PDB: 2BVL) (red), reactive $loop_{510–523}$ (blue), UDP-glucose (green). (D) Structural alignment of TcdB GTDs from B1, B2, and B3 subtypes, the reactive $loop_{510–523}$ is highlighted. (E) Sequence alignment of reactive $loop_{510–523}$ of TcdB subtypes and TcdA1 reactive $loop_{509–522}$, colored by homology. Panel B made with biorender.com.

Baldwin 2015; P. Chen and Jin 2023). Additionally, a subset of TcdB variants has extensive residue changes these sites, enabling them to escape neutralization (Mansfield et al. 2020) (Figure 1A). This accounts for the 200-fold reduced potency of Bezlotoxumab against TcdB variants in approximately 15%–20% of strains and the complete escape of TcdB in hypervirulent RT017 strains from a preclinical mAb, PA41, neutralization (Hernandez et al. 2015; Mansfield et al. 2020; Marozsan et al. 2012). The evolution of human α-defensins that neutralize GTDs of TcdA and TcdB by aggregation or enzymatic inhibition highlights the feasibility of this approach (Giesemann et al. 2008; Korbmacher et al. 2020; Fischer et al. 2020; Barthold et al. 2022).

Responding to the urgent need for novel modalities to treat CDI, we propose a novel approach that leverages peptides to inhibit the virulence factors TcdA and TcdB by binding to their conserved glucosyltransferase catalytic site (GTD). As the key catalytic residues and UDP-glucose pocket of the GTD are highly conserved between toxin variants of both TcdA and TcdB (Mansfield et al. 2020) (Figure 1C–E), inhibitors of their active sites are in fact likely to have broad activity against many clinically relevant *C. difficile* strains. This approach is also compatible with the current standard of care antibiotics, poses minimal risk for drug resistance development, and targets toxin variants from at least 90% of clinical *C. difficile* isolates.

In previous works (Xiao et al. 2022; Sarma et al. 2023), we provided a proof of concept of this approach by improving peptide inhibitors of TcdA GTD found in the literature via iterative computational evolution (Xiao et al. 2022; Sarma et al. 2023; Abdeen et al. 2010). In this study, we turned to TcdB, a more challenging and clinically relevant target due to its higher sequence diversity (Mansfield et al. 2020; E. Shen et al. 2020), higher glucosyltransferase activity (Chaves-Olarte et al. 1997), and direct role in driving fulminant CDI (Carter et al. 2015; Lyras et al. 2009). We leveraged our background technology portfolio including (i) a microfluidic device for the rapid identification of peptide binders (Kilgore et al. 2023; Day et al. 2019; Saberi-Bosari et al. 2019), (ii) an in silico workflow that combines *pep*tide *b*inding *d*esign (*PepBD*) and MD simulations to enhance peptide-protein affinity, (iii) glucosyltransferase inhibitor screening, (iv) peptide-protein binding studies, and (v) a translatable primary human small intestine and colon monolayer model (Ok et al. 2023) to identify broad-spectrum peptide inhibitors of *C. difficile* TcdB.

2 | Results

2.1 | De Novo Peptide Discovery Through Solid Phase Peptide Library Screening

The TcdA and TcdB GTDs contain a binding pocket for UDP-glucose which our team previously targeted for the design of TcdA peptide inhibitors (Xiao et al. 2022; Sarma et al. 2023). Contained within the pocket are two highly conserved catalytic regions, a tryptophan residue (W102) that binds to the uracil of UDP-glucose through π–π stacking and the DXD motif (D286/D288), which coordinates with a magnesium or manganese ion co-factor (Aktories et al. 2017; Jank et al. 2007). The pocket is partially covered by a flexible reactive loop (W520 loop, residues 510–523), which undergoes a large conformational rearrangement upon UDP-glucose and Mn^{2+} binding, allowing it to mediate the binding and orientation of Rho proteins for glucosylation (Liu et al. 2021; Pruitt et al. 2012).

Our previous studies indicated that the optimal peptide length for binding in this pocket is eight amino acids, thus informing the design of a solid-phase peptide library for the de novo discovery of TcdB GTD-inhibiting peptides: $X_1X_2X_3X_4X_5X_6X_7X_8$-GSG-resin. The eight variable positions (X_n) were randomized with a focused ensemble of chemically diverse amino acids: alanine (A), aspartic acid (D), phenylalanine (F), proline (P), glutamine (Q), arginine (R), threonine (T), and tryptophan (W), which encompass a wide range of interactions (i.e., electrostatic, hydrogen-bonding, hydrophobic, π stacking, etc.) thereby promoting the identification of sequences with true affinity for TcdB GTD. The peptide library was synthesized on ChemMatrix aminomethyl resin via Fmoc/tBu chemistry following the "split-couple-recombine" technique, yielding a unique peptide sequence on each resin bead. We then screened the library by implementing a bichrome assay on a high-throughput microfluidic-microscopy device to select peptides with TcdB GTD targeting activity (Figure 2A). Briefly, the library beads were (i) contacted with a solution of red fluorescently labeled TcdB (TcdB-AF594) and green-fluorescent analog of UDP-glucose (UDP-glucose-fluorescein); (ii) individually fed to the sorting chamber of the device; and (iii) imaged in both red and green channels. The collected images were processed in real-time to extract bead image metrics that determined bead collections: beads with high red-only fluorescence—indicating selective TcdB targeting and inhibition of UDP-glucose binding—were selected; beads with red *and* green fluorescence—indicating TcdB-binding, yet not inhibitory, sequences—or no fluorescence were discarded. Out of approximately 5000 beads screened, 69 positive leads were captured, 36 of which were sequenced by Edman degradation, obtaining 28 sequences with high confidence. Notably, the identified sequences showed significant enrichment in arginine (R) (X_1–X_8), glutamine (Q) (X_1–X_7), and proline (P) (X_1–X_8) as well as high sequence similarity for arginine (R) at position X_2, and glutamine (Q) at positions X_1 and X_4 (Figure 2A, inset). Interestingly, the QR motif was observed 15 times in the sequences, and the motif QRP and its reverse PRQ were found in 4 and 2 sequences, respectively. Previous work with TcdA by us and others similarly found an enrichment for the positively charged residues arginine or histidine (Xiao et al. 2022; Sarma et al. 2023; Abdeen et al. 2010). Six sequences were selected for their selective and inhibitory TcdB targeting, high confidence sequencing, and homology (Figure 2B; all sequences provided in the Supporting Information).

2.2 | Computational Evaluation of the Binding Affinity of Library-Designed Peptides for TcdB GTD

The binding energy ($\Delta G_{binding}$) of peptides LSB1–LSB6 for the catalytic site on TcdB1 GTD was initially evaluated via peptide:protein docking followed by molecular dynamics (MD) simulations. The peptides were docked against the reactive loop (residues 510–523) and the DXD motif (residues 286–288)

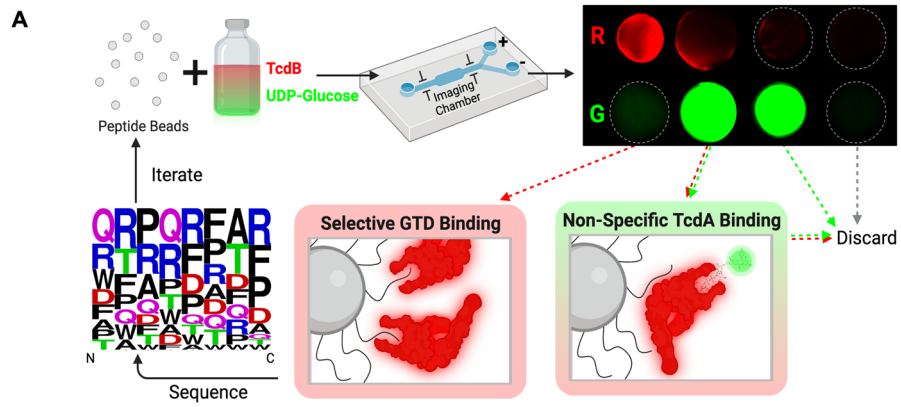

B

Peptide	Sequence	Binding Estimate
LSB1	RPDQRTAP	-5.68 ± 0.65
LSB2	AQQRFAPF	Does not bind (ΔG > 0)
LSB3	ATRTTDFF	Does not bind (ΔG > 0)
LSB4	FWTPFTQP	Does not bind (ΔG > 0)
LSB5	QRPQQRTF	-5.70 ± 0.54
LSB6	QRPAPQTR	-1.62 ± 0.34

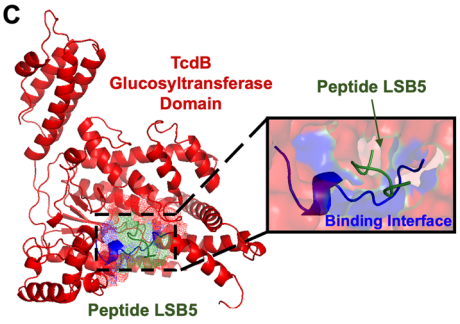

FIGURE 2 | Solid phase peptide library screening. (A) A solid phase peptide library was screened against TcdB holotoxin (red) and UDP-glucose-fluorescein (green) to select peptides with selective and inhibitory TcdB GTD activity. Library beads exhibiting red-only fluorescence were selected as carriers of peptides capable of displacing UDP-glucose-fluorescein upon binding TcdB GTD. (B) The selected beads were analyzed via Edman degradation, and the resulting sequences LSB1–LSB6 were modeled via molecular docking and dynamics simulation on the UDP-glucose binding pocket of TcdB GTD to estimate the binding free energy $\Delta G_{\text{binding}}$ (*note:* the values of energy were averaged from triplicate docking and 100-ns dynamic simulations in explicit solvent conditions). (C) Snapshot of the LSB5:TcdB GTD complex resulting from molecular dynamics simulation, with the TcdB GTD in red, reactive loop in blue, and peptide LSB5 in green.

(Reinert et al. 2005) of TcdB1 GTD using the docking software HADDOCK (v. 2.4) and clustered based on the fraction of common contacts (Honorato et al. 2024; van Zundert et al. 2016). The top binding pose of the first cluster of each peptide:TcdB1 GTD complex was selected for further MD refinement and $\Delta G_{\text{binding}}$ evaluation. Three independent 100 ns simulations for each peptide:TcdB1 GTD complex were carried out. The implicit-solvent molecular mechanics/generalized Born surface area (MM/GBSA) approach with the variable internal dielectric constant model was used to evaluate the $\Delta G_{\text{binding}}$ from the last 5 ns of the simulation trajectories, summarized in the table within Figure 2B. Three peptides were predicted to bind weakly near the reactive loop: LSB5, LSB1, and LSB6, all of which are basic and contain the QR-motif.

2.3 | In Silico Optimization of Peptide Binders for TcdB GTD

We then applied the PepBD algorithm, coupled with atomistic MD simulations, to optimize the GTD inhibitory activity of the peptide sequences identified by library screening. PepBD (*Pep*tide *B*inding *D*esign) is a Monte-Carlo-based search algorithm that uses an iterative procedure to identify variants of a reference sequence that may bind with superior affinity to a biomolecular target. The input to the algorithm is a crystal structure of the complex formed by the target protein and the reference peptide, herein the TcdB1 GTD (PDB ID: 2BVL) and LSB sequences. The algorithm performs two kinds of moves: sequence change and conformation change moves, to generate peptide variants. After each move, the algorithm calculates a score (a measure of the peptide-receptor binding energy and the conformational stability of the peptide when bound to the receptor); this score is compared to that of the previous sequence/conformation and accepted or rejected using the Monte Carlo Metropolis sampling technique. Details of the algorithm are provided in the Methods and Supplementary Information (Xiao et al. 2022, 2018; Sarma et al. 2023). The evaluation of the ΔG values follow the same protocol as in our previous work (Xiao et al. 2016).

Peptide LSB5 (QRPQQRTF) was indicated by initial simulations to be the best binder to TcdB1 GTD ($\Delta G_{\text{binding}} = -5.7$kcal/mol) and the LSB5:TcdB1 GTD complex (Figure 2C) was therefore adopted as the starting point for the PepBD optimization. For our designs, we considered three different design spaces (Cases) for PepBD where we constrained the number of hydrophobic, hydrophilic, cationic, anionic, and glycine residues on the peptide chain. These constraints facilitated the search for soluble peptides with high target-binding affinity. For example, the number/position of charged amino acids was fixed to complement the charge state of the catalytic site of TcdB1 GTD. The three cases are listed in Supporting Information S1: Table S2. Broadly, Cases 1 and 2 have amino acid distributions that are similar to successful TcdA GTD peptide inhibitors, that is, they are biased towards hydrophobic and charged residues, whereas

Case 3 has the same hydration properties as the reference peptide LSB5. For Cases 1 and 2, we performed the PepBD search with two randomized initial peptide sequences to explore different search pathways, whereas for Case 3 the search started from LSB5. In each search, new peptide sequences and conformers were generated and the Γ_{score} and RMSD were recorded at each step (Figure 3A–D), where a lower Γ_{score} indicates stronger binding. The lowest scoring peptides were subjected to atomistic MD simulations to predict their binding affinity as described above (Table 1). The structures of the SB2:TcdB1 GTD, SB5:TcdB1 GTD, and SB6:TcdB1 GTD complexes obtained by performing a hierarchical clustering analysis on the last 5 ns of a 100 ns simulation are shown in Figure 3E–G.

Notably, top Case 2 sequences SB1, SB2, SB5, and SB6 share a C-terminal WRRW motif, and residue-wise analyses of SB2, SB5, and SB6 also reveal that R6, R7, and W8 are the highest contributors to the interaction energy (Figure 3E–G). Decomposition of energy terms reveals that the arginine residues contribute through a mix of van der Waals (VDW), electrostatic, and polar solvation, whereas the tryptophan residues contribute primarily through VDW. Taken together, these results show a substantial improvement in $\Delta G_{binding}$ during in silico optimization, coupled with convergence toward similar peptide sequences. These peptides are distinct from previously reported TcdA and TcdB GTD-inhibiting peptides. While they all are positively charged and 7–10 amino acids in length, these interact with the GTD active site through their C-terminal WRRW motif (Xiao et al. 2022; Sarma et al. 2023; Abdeen et al. 2010).

2.4 | Broad Spectrum Glucosyltransferase Inhibition

Encouraged by the in silico improvement in $\Delta G_{binding}$ to TcdB1 GTD, we sought to investigate the matured peptides' glucosyltransferase (GT) inhibition activity in vitro against a panel of TcdB variants. Recent advances in the field have classified and characterized up to 12 distinct variants of TcdB, with numerous subtypes (Mansfield et al. 2020; E. Shen et al. 2020). Their GTDs exhibit high sequence diversity (Mansfield et al. 2020; E. Shen et al. 2020) and have distinct Rho protein substrate preferences (Genth et al. 2014; Liu et al. 2021), contributing to different cell-rounding effects (Genth et al. 2014) and limiting the universality of GT inhibitors. While the three key catalytic residues (W102, D286, D288) are conserved across all strains reported on DiffBase (Mansfield et al. 2020), the UDP-pocket and reactive loop are only moderately conserved (Figure 1E), while the Rho protein-binding interface partitions into two functional groups, RhoA (TcdB1, B2, B5, B6, B9, B10, B11, and B12) and R-Ras (B3, B4, B7, and B8) (Liu et al. 2021). Despite distinct Rho protein preferences, both groups retain the ability to glucosylate Rac1 with similar activity, allowing us to probe the GT activity in both groups

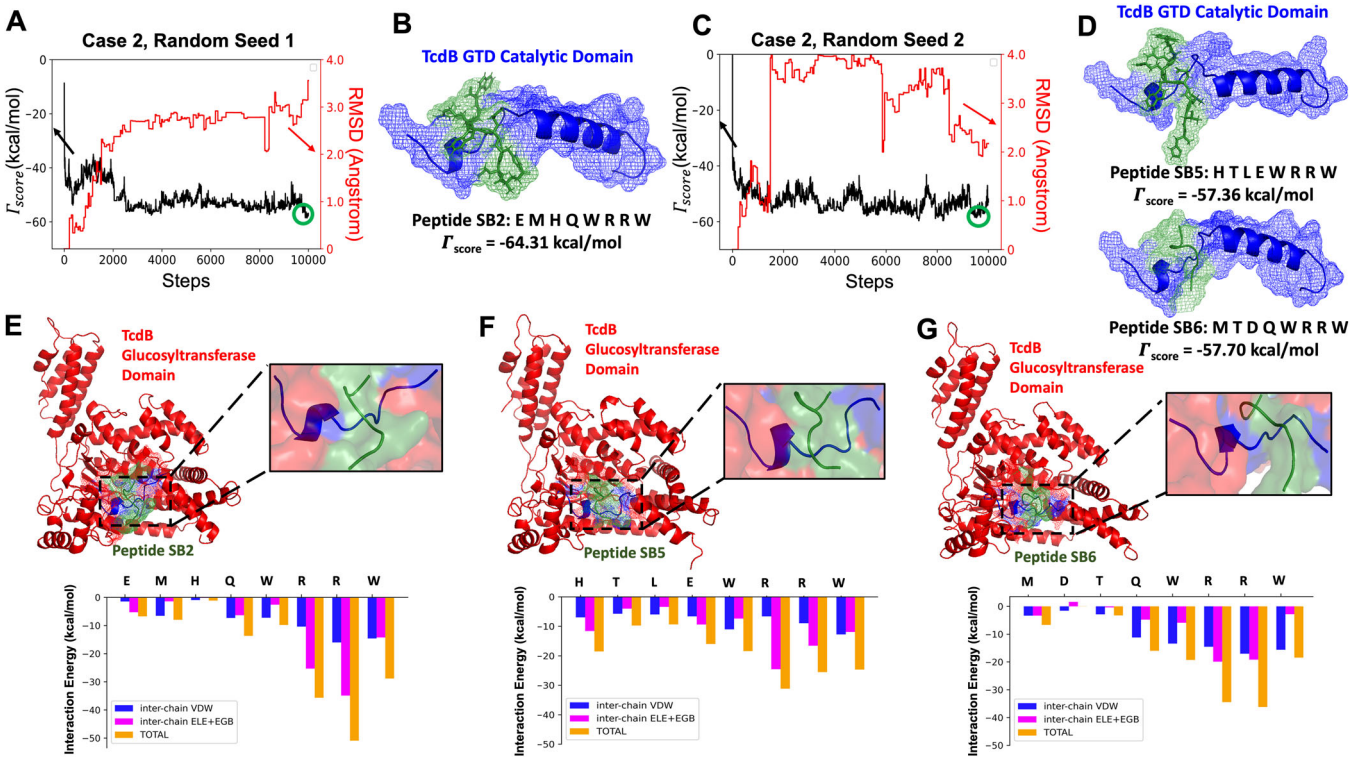

FIGURE 3 | Peptide sequences SB2, SB5, and SB6 were obtained from PepBD and molecular dynamics simulations. (A) The score/RMSD versus the number of sequence and conformation steps for Case 2 (random seed 1) results in (B) peptide SB2 (sequence: EMHQWRRW). Similarly, (C) the score/RMSD plot for Case 2 (random seed 2) and the two lowest scoring peptides, (D) SB5 (sequence: HTLEWRRW) and SB6 (sequence: MTDQWRRW). Snapshots of peptides (E) SB2, (F) SB5, and (G) SB6 bound to TcdB GTD obtained from molecular dynamics simulation and their corresponding residue-wise decomposition of their interaction energies (van der Waals + Electrostatic + Polar solvation energy contribution). Green circles in (A) and (C) indicate the Steps at which SB2, SB5, and SB6 were identified.

TABLE 1 | The initial peptide sequence (LSB5) and the list of peptide sequences identified by PepBD screening with their corresponding $\Delta\Gamma_{score}$ and $\Delta G_{binding}$ values with standard error (SE) ($n = 1250$ snapshots).

Peptide	Case	Sequence	$\Gamma_{score}\left(\frac{kcal}{mol}\right)$	*predicted* $\Delta G_{binding}\left(\frac{kcal}{mol}\right)$
LSB5		QRPQQRTF		-5.7 ± 0.54
SB1	Case 2	FDQQWRRW	−58.64	-25.33 ± 0.38
SB2	Case 2	EMHQWRRW	−64.31	-20.07 ± 0.50
SB3	Case 1	GWQEWRTW	−59.66	-16.41 ± 0.42
SB4	Case 3	PRHQNRFH	−56.94	-15.35 ± 0.50
SB5	Case 2	HTLEWRRW	−57.36	-14.83 ± 0.58
SB6	Case 2	MDTQWRRW	−57.70	-14.08 ± 0.42
SB7	Case 3	RAHQNRFH	−57.30	-7.51 ± 0.51

using the same substrate (Genth et al. 2014; Liu et al. 2021). TcdB1 (VPI 10463), B2 (R20291), and B3 (1470) were selected for coverage across both Rho protein functional groups, presence in key hypervirulent strains of interest, and high abundance (~90%) in clinical isolates.

The panel of computationally optimized peptides (SB1–SB7) and the reference peptide (LSB5) were evaluated as candidate inhibitors of TcdB1, B2, and B3 GTDs using a luminescence-based glucosyltransferase assay, UDP-Glo (Promega). The rate of product (UDP) formation was measured following conventional protocols (Barthold et al. 2022; Liu et al. 2021; Heber et al. 2022). Castanospermine (Cast), an established glucosidase and glucosyltransferase inhibitor with activity against TcdB, was used for comparison (Heber et al. 2022; Jank et al. 2008). At fixed inhibitor (1 mM) and Rac1 (5 μM) concentrations and varied UDP-glucose concentration, peptides SB2, SB5, and SB6 demonstrated robust inhibitory activity against all three TcdB GTD variants (Figure 4). Interestingly, the three peptides have the same hydration properties (Case 2) and share the C-terminal WRRW motif. One other peptide, SB1, has the same characteristics but noticeably reduced GT inhibition activity, possibly due to the N-terminal bulky phenylalanine residue. Peptides from Case 3: SB4, SB7, and LSB5, exhibited no inhibitory activity, whereas the remaining peptide, SB3, from Case 1, represented only a modest inhibitory activity. Case 3 peptides had more hydrophilic residues (4 vs. 2), and fewer hydrophobic residues (1 vs. 3) than both Cases 1 and 2. Peptides therefore exhibited hydration-dependent activity in vitro, progressing in the order Case 2 > Case 1 > Case 3 (Table 1). While the optimal hydration properties are difficult to predict a priori, these results are congruent with the sequence-activity relationship of peptide inhibitors designed in silico against the TcdA GTD (Sarma et al. 2023).

2.5 | Peptide Inhibition of Rho Glucosyslation Through Direct Competition

The TcdB GTD is a retaining glucosyltransferase that follows a stepwise substitution nucleophilic internal (S_Ni) mechanism through the formation of a ternary complex with UDP-glucose and Rho proteins (Paparella et al. 2022). The crystal structures of toxin GTDs with UDP, UDP-glucose, and Rho proteins imply a sequential binding of UDP-glucose first and then Rho proteins (Liu et al. 2021; D'Urzo et al. 2012). Previous studies investigating the effects of TcdB GTD inhibitors measured the apparent reaction velocities using fixed Rho protein concentrations and only varied UDP-glucose (Barthold et al. 2022; Heber et al. 2022; Tam et al. 2015; Paparella et al. 2021). This reasonable simplification of the reaction mechanism views the inhibitor as disrupting primarily the hydrolysis or transfer of UDP-glucose, as is the case for transition state analogs and other small-molecule inhibitors. As the in silico GTD:peptide complexes indicate that the peptides primarily contact the reactive loop over the UDP-glucose pocket, multiple inhibition mechanisms are possible, namely direct competition or allosteric modulation with UDP-glucose, competition with Rho proteins, or more complex mixed modes of inhibition with either substrate (Equation 1). Thus, we propose a compulsory ordered Bi–Bi, two reactant–two product, reaction mechanism with six possible mechanisms of inhibition (Equation 1, Supporting Information S1: Table S3) (Paparella et al. 2022; Segel 1935; Copeland 2023).

$$\begin{array}{ccccc} E + \mathrm{UDP-glc} & K_{\mathrm{UDP-glc}} \leftrightarrow & E \cdot \mathrm{UDP-glc} + \mathrm{Rho} & K_{\mathrm{Rho}} \leftrightarrow & E \cdot \mathrm{UDP-glc \cdot Rho} \rightarrow E \cdot \mathrm{UDP} + \mathrm{Rho-glc} \\ + & & + & & + \\ I & & I & & I \\ \updownarrow K_I & & \updownarrow \alpha K_I & & \updownarrow \alpha\beta K_I \\ E \cdot I + \mathrm{UDP-glc} & \alpha K_{\mathrm{UDP-glc}} \leftrightarrow & E \cdot \mathrm{UDP-glc} \cdot I + \mathrm{Rho} & \beta K_{\mathrm{Rho}} \leftrightarrow & E \cdot \mathrm{UDP-glc \cdot Rho} \cdot I \end{array} \quad (1)$$

The mechanisms of inhibition of SB2, SB5, SB6, and Cast were determined by assessing inhibitory activity at varied concentrations of both substrates, UDP-glucose and Rac1. These inhibitors display dose-dependent activity but differ in their response to each substrate. Cast favors the UDP-glucose bound state and is uncompetitive with respect to Rac1, which is consistent with the previous literature describing iminosugar

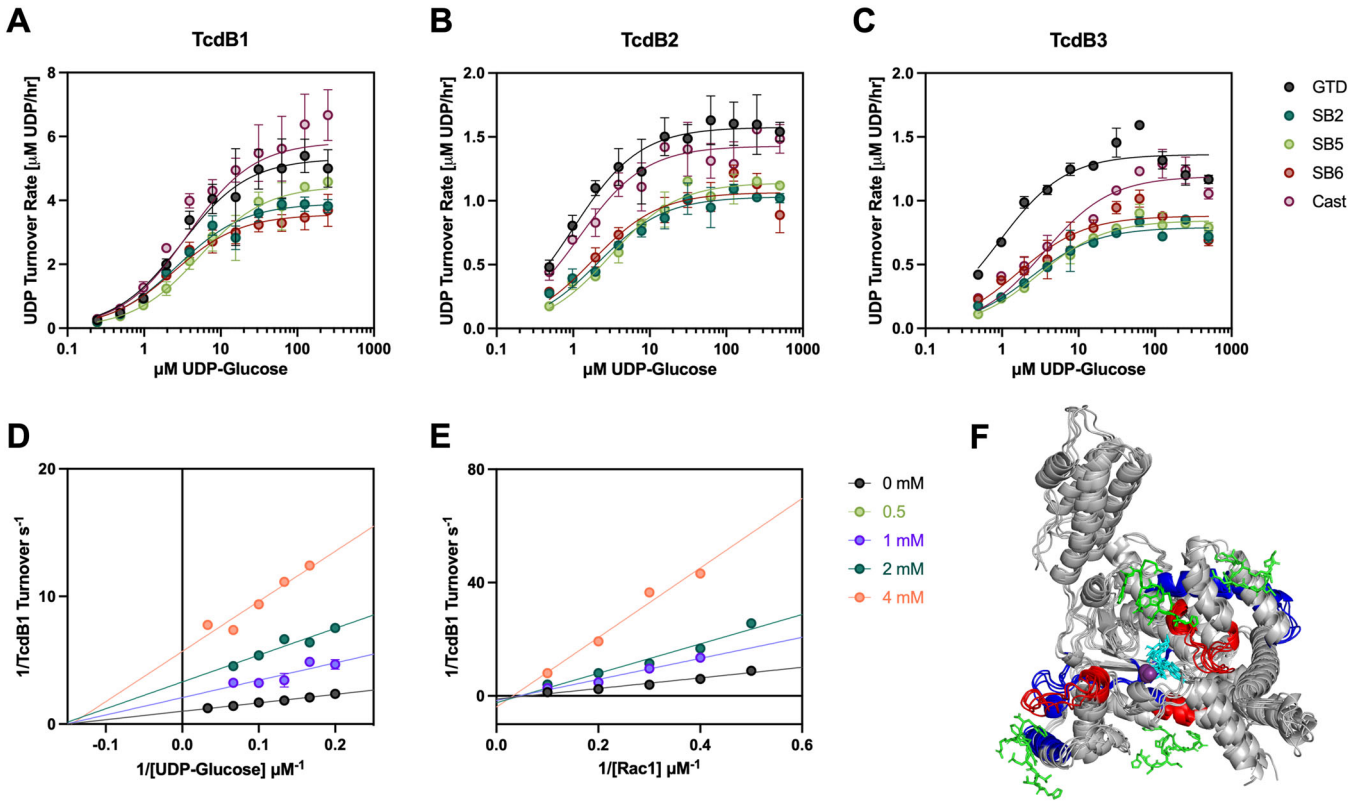

FIGURE 4 | Peptides demonstrated broad glucosyltransferase inhibition by blocking Rho-protein binding. (A–C) Peptides were screened for inhibitory activity against TcdB1, B2, and B3 GTDs. Glucosyltransferase activity was measured at 10 nM TcdB GTD, 1 mM inhibitor, 5 μM Rac1, and varied UDP-glucose concentrations. Inhibition data were fit to the mixed inhibition mode equation (GraphPad Prism). Inhibitor curves for SB2 (dark teal), SB5 (green), SB6 (red), and Cast (purple) are shown for (A) TcdB1 GTD, (B) TcdB2 GTD, and (C) TcdB3 GTD. Raw data for all inhibitors tested can be found in the Supporting Information. (D, E) Peptides SB2, SB5, and SB6 are noncompetitive inhibitors with respect to UDP-glucose and competitive inhibitors with respect to Rac1. Lineweaver–Burk plots for (D) 0–30 μM [UDP-glucose] and (E) 0–10 μM [Rac1] for SB6 and TcdB1 GTD are shown with linear regressions for illustration. The concentration of the complementary substrate was fixed at 5 μM. Relevant parameters, including K_i and K_M, were calculated from nonlinear regressions of the non-transformed data. TcdB GTDs $n = 4$, TcdB GTDs + inhibitor $n = 2$, free UDP converted to 1/enzyme turnover, means ± SD. Some error bars are smaller than data point symbols and therefore are not explicitly shown. (F) Changes in TcdB 1 GTD (PDB: 7S0Y) (gray ribbon) solvent exposure upon SB5 binding determined by hydrogen–deuterium exchange mass spectrometry (HDX-MS), where red indicates less solvent exposure (binding) and blue indicates more solvent exposure (conformational change). HADDOCK docking and MD simulation show potential conformations of the SB5 peptide (green) on TcdB1 GTD at the three putative binding sites, thus supporting the direct Rho competition inhibition mechanism.

transition state analog inhibitors (Paparella et al. 2022, 2021). Iminosugar inhibitor binding substantially increases with the presence of UDP in the binding pocket and they exert their inhibitory activity by mimicking the glucocationic transition state, acting only on the quaternary complex (Supporting Information S1: Figure S6) (Jank et al. 2008; Paparella et al. 2021). In contrast, the peptides displayed noncompetitive and competitive inhibition patterns with varied concentrations of UDP-glucose and Rac1, respectively (Figure 4C–E and Supporting Information S1: Figures S4 and S5). These patterns indicate that the peptides directly compete with Rho proteins by targeting both the free GTD and GTD:UDP-glucose complex, thus preventing Rho protein binding and blocking glucosyltransferase activity (Supporting Information S1: Table S2). This is distinct from previously reported peptides whose inhibitory activity against TcdB1 is inferred to be competitive with respect to UDP-glucose (Abdeen et al. 2010).

The inhibition constants K_i and the weighting parameters α and β were determined by fitting to Equation (2), the reaction rate equation for an ordered Bi–Bi reaction (Table 2, derivation provided in the Supporting Information). The peptides' activity towards different GTD:substrate(s) complexes is reflected in their weighting parameters. The three peptides exhibit $\alpha > 1$ and $\beta \gg 1$, where α slightly greater than one indicates a preference for the free GTD over the GTD:UDP-glucose complex, while $\beta \gg 1$ indicates that no quaternary complex forms. These results are consistent with the design optimization towards the free GTD, suggesting that the peptides inhibit the glucosyltransferase activity of TcdB only before Rac1 binding to GTD.

$$v = \frac{V_{\mathrm{Max}}[\mathrm{UDP-glc}][\mathrm{Rho}]}{K_{\mathrm{UDP-glc}}K_{\mathrm{Rho}}\left(1+\frac{[I]}{K_I}\right)+K_{\mathrm{Rho}}[\mathrm{UDP-glc}]\left(1+\frac{[I]}{\alpha K_I}\right)+[\mathrm{UDP-glc}][\mathrm{Rho}]\left(1+\frac{[I]}{\alpha\beta K_I}\right)}. \quad (2)$$

TABLE 2 | Inhibitor parameters fit to Equation (2) for a Bi–Bi reaction mechanism.

	K_i [μM]			Alpha			Beta		
Inhibitor	**TcdB1**	**TcdB2**	**TcdB3**	**TcdB1**	**TcdB2**	**TcdB3**	**TcdB1**	**TcdB2**	**TcdB3**
SB2	618	919	2413	2.9	6.5	12	1244	393	528
SB5	125	188	163	4.1	7.4	1.7	1142	1142	2219
SB6	832	729	2696	1.1	3.2	2.0	550	287	994
Cast	7115	2348	3885	798	767	30	0.00020	0.00024	0.0024

Note: K_i is the inhibition constant, alpha is the weighting parameter on the GTD:UDP-glucose and GTD:UDP-glucose:Rac1terms, and beta is the weighting parameter on the GTD:UDP-glucose·Rac1term.

The inhibition constants, K_i, for each peptide varied up to fourfold between TcdB GTD sub-types. SB5 demonstrated the most robust inhibition and least variation between subtypes with $K_{i,SB5,avg} = 0.16 \pm 0.04$ mM. SB2 and SB6 exhibited similar inhibitory activity against TcdB1 and TcdB2 GTDs, with a K_i of 0.62–0.92 mM, but a fourfold lower activity against the TcdB3 GTD, with $K_{i,SB2:B3} = 2.4$ mM and $K_{i,SB6:B3} = 2.7$ mM. Because the TcdB1 GTD was used as the target for both the peptide library screening and the in silico optimization, it is not surprising that the peptides demonstrated higher inhibition of the GTDs of TcdB1 and TcdB2, which belong to the same Rho-family and share significant homology compared to the TcdB3 GTD.

Here we are the first to report distinct Michaelis constants, K_M, for UDP-glucose and Rac1 for all three TcdB GTDs. The Michaelis constant for UDP-glucose, $K_{M,UDP\text{-}glc}$, was found to be 8.0 μM, consistent with previously reported apparent K_M^{app} of 3.8–16 μM for the TcdB1 GTD (Liu et al. 2021; Loughney et al. 2017). Similarly, the $K_{M,UDP\text{-}glc}$ for the TcdB2 and TcdB3 GTDs were found to be 5.7 and 6.0 μM, respectively. Since $K_{M,UDP\text{-}glucose}$ is much lower than the physiologic concentration of UDP-glucose, we expect the GTD to be saturated by the substrate intracellularly. This may limit the inhibitory efficacy of the peptides as they exhibit a slight preference for the unbound GTD ($\alpha > 1$). In contrast, the Michaelis constants of Rac1 for each GTD, $K_{M,Rac1}$, are higher (i.e., 66, 32, and 31 μM, respectively), indicating that most of the toxin is in the GTD:UDP-glucose state, which does not impair peptide blockade of Rac1 binding.

2.6 | HDX-MS Epitope Mapping Confirms Rho-Interface Blockade

Hydrogen–deuterium exchange mass spectrometry (HDX-MS) was used to identify SB5 binding epitopes on the TcdB1 GTD and assess the subsequent conformational changes (Song et al. 2015; B. Chen et al. 2022). Three regions of TcdB1 GTD showing significant decreases in deuterium uptake at 1- and 10-min timepoints indicated SB5-binding sites (Figure 4F and Supporting Information S1: Table S4 and Figure S7). One site is located at the Rho-binding interface near residues 453–467 (Site 1), adjacent to the UDP-glucose-binding pocket and opposite to the reactive loop (510–523). This binding site supports the observed inhibition activity of blocking Rho-protein binding. Additionally, there is a corresponding conformation change behind this region at residues 398–423, which becomes more solvent-exposed when SB5 is bound (Supporting Information S1: Table S4 and Figure S7). Coverage limitations prevented the direct measurement of deuterium exchange at the reactive loop (510–523) and α16–17 helices (424–437 and 444–450) (Liu et al. 2021; Centers for Disease Control and Prevention U.S. 2019), which are not precluded from also interacting with the peptide, given the spatial proximity. Two additional binding regions were identified near residues 224–230 (Site 2) and 297–310 (Site 3). SB5 binding to Site 2 increased the solvent exposure of residues 229–244, while binding to Site 3 induced local conformational changes at surrounding residues 285–296, 341–352, and 356–362.

To determine how well SB5 may bind to the HDX-MS determined sites, we docked and performed MD simulations of SB5 to four a priori regions: the reactive-loop/active-site pocket (286–288, 510–523) and three HDX-defined surfaces (Site 1: 453–467; Site 2: 297–310; Site 3: 224–230). In total, we performed 14.7 μs of MD simulation (see Methods). From the initial design, SB5 bound strongly to the active site of TcdB1 ($\Delta G_{binding} = -14.83 \pm 0.58$ kcal mol^{-1}). SB5 also engaged Site 1 at the Rho interface in many potential conformations in the apo and UDP-glucose bound TcdB with $\Delta G_{binding}$ ~−10 to −4 kcal mol^{-1}. Selected conformations of the peptides are shown in Figure 4F along with the primary binding regions detected by HDX-MS. SB5 showed strong interaction at Site 2 (-7.39 ± 1.50 kcal mol^{-1}) and minimal interaction at Site 3 (-0.74 ± 1.29 kcal mol^{-1}). As a control, a scrambled peptide ScSB5 (Sequence: RHWLRETW) was evaluated at the apo active site of TcdB1. ScSB5 showed weaker binding (-3.99 ± 1.36 kcal mol^{-1}; Supporting Information S1: Figure S8) than SB5, suggesting that SB5's inhibitory activity reflects sequence-specific interactions at the loop/active-site pocket rather than nonspecific electrostatics. We also applied the same protocol to SB5 at the TcdB3 active site, supporting this conclusion, as SB5 bound to the active loop of TcdB3 with a moderate binding energy (-6.99 ± 1.42 kcal mol^{-1}; Supporting Information S1: Figure S8). Full data of SB5 and ScSB5 and the various conformations and binding affinity tests can be found in the Supporting Information. The HDX-MS epitope mapping combined with additional peptide docking and MD simulations further support the proposed inhibitory mechanism. SB5 interacts strongly with the active site of the GTD without UDP-glucose bound (apo), and with Site 1 on the Rho binding interface with and without UPD-glucose present, enabling noncompetitive inhibition with respect to UDP-glucose and competitive inhibition with respect to Rho-proteins.

2.7 | Peptides Delay Toxin-Mediated Cytotoxicity in Primary Human Colonocytes

Peptides LSB5, SB2, SB5, SB6, and SB7 were evaluated for neutralization activity in a human colon epithelial (hCE) culture system, which served as a functional model of toxicity (Sarma et al. 2023; Ok et al. 2023). This system is highly sensitive to exposure to *C. difficile* toxins and recapitulates the relevant human in vivo characteristics, including barrier function and gene expression profiles (Ok et al. 2023). The hCE monolayers were established by growing colonic epithelial stem cells to confluence on the permeable membrane of a transwell, followed by differentiation into the primary absorptive lineage, which is the cell type most exposed to *C. difficile* toxins. This differentiation process promotes tight junction formation, reducing ion flux and increasing the trans-epithelial electrical resistance (TEER) (Sarma et al. 2023; Ok et al. 2023). Upon exposure to a basal concentration of 30 pM TcdB1 (TcdB), typical in patients' stool (P. Chen et al. 2019), there was a rapid decline of TEER and an increase in apoptosis within 6–24 h. The peptides were incubated with the hCE monolayers 1 h before the TcdB challenge and TEER was monitored over 26 h (Figure 5A). Apical and basal exposure to TcdB resulted in a 50% reduction in TEER within 10 h. Peptides SB2, SB5, and SB6 delayed TEER loss by 4.1, 4.9, and 6.0 h, respectively. Notably, LSB5, which showed only a modest glucosyltransferase inhibition, delayed TEER loss by 5.6 h. Interestingly, the extent of the delay in TEER loss did not directly correlate with the peptides' K_i, suggesting that multiple factors influence activity in vitro. Subsequently, the monolayers were stained for cleaved-caspase 3 (CC3), a marker of apoptosis, 26 h after exposure to TcdB (Figure 5B,C). SB2, SB5, SB6, and LSB5 showed a significantly lower CC3 signal than the TcdB control, indicating protection from TcdB-mediated apoptosis. Conversely, SB7, which showed negligible glucosyltransferase inhibition, did not delay TEER loss nor decrease the apoptosis compared to the TcdB control. The peptides optimized in silico—SB2, SB5, and SB6—demonstrated an activity consistent with their proposed mechanism, preventing Rho glucosylation and blocking the final step in the TcdB intoxication pathway, thereby maintaining cytoskeleton integrity and reducing apoptosis. Among them, SB6 provided the largest delay in TEER loss and the smallest apoptosis signal, which contrasts with the relative efficacy of SB5 over SB6 observed in the glucosyltransferase inhibition studies. The more complex and physiologically relevant conditions of the hCE monolayer pose greater barriers to effective neutralization by the peptides. Differences in activity may be attributed to variances in protease resistance, cell penetration, diffusion, or the interaction between the peptides and other biologics in the transwell environment.

3 | Discussion

The development of effective therapies against CDI remains an urgent medical need. In this study, we identified and computationally evolved a set of novel TcdB GTD-inhibiting peptides via combinatorial selection and in silico optimization, followed by screening for inhibitory activity against three TcdB subtypes. We then elucidated the mechanism of inhibition, showing that these peptides competitively bind to the Rho protein binding site of the GTD. Further, we tested these peptide inhibitors in a primary hCE model, demonstrating their ability to prevent TcdB-mediated cell rounding and cytotoxicity. The reported Michaelis constants, K_M, for both substrates, UDP-glucose and Rho proteins, for three TcdB GTD subtypes, provide new mechanistic detail that will aid the development of future glucosyltransferase inhibitors. While the translational potential of these peptides is limited by their modest affinity, their robust characterization through novel enzymatic, biochemical, and primary hCE assays lays the foundation for novel therapeutics against CDI.

The differential cross-reactivity of these peptide inhibitors across the three TcdB subtypes examined underscores the challenge of developing a potent, broad-spectrum inhibitor. Of the peptides tested, only SB5 maintained comparable activity against the TcdB3 GTD (R-Ras binding family) as the TcdB1 and TcdB2 GTDs (RhoA binding family). Three key substitutions in the reactive loop (S511A, M516K, and A517N) and additional changes in the α16–17 helices underlie the distinct Rho protein selectivity of these families (Liu et al. 2021) and likely explain the reduced activity of SB2 and SB6 toward TcdB3. Elucidating the structural features that enable SB5 to tolerate these substitutions could inform future peptide optimization efforts. Notably, the reactive loop of the TcdA GTD is highly homologous to both TcdB families, but, two of these three residues also differ (L510S/A and I516M/K in TcdA vs TcdB1/B3), contributing to TcdA's distinct Rho protein specificity (Genth et al. 2014; B. Chen et al. 2022). Investigating the cross-reactivity of these peptides against the TcdA GTD is warranted, although these structural differences may limit their activity.

The mechanism by which these peptides enter cells remains unclear. In the intact holotoxin, the catalytic site and Rho binding interface of the GTD are partially occluded by the CPD and only become exposed upon CPD-mediated cleavage into the cytosol (A. Shen et al. 2011; P. Chen et al. 2019). This suggests that the peptides cannot bind to the GTD extracellularly and exert their protective effect through one of three plausible mechanisms (i) independently entering the cytosol to block GTD activity, (ii) associating with other domains of the holotoxin to hitchhike into the cell and inhibit the GTD, or (iii) binding to receptor-binding domains to prevent toxin uptake altogether. Because our modeling and mechanistic studies focused solely on the GTD, it remains unclear whether the peptides interact with other toxin domains. Nonetheless, their inhibition of GTD activity in vitro suggests that their protective effect in hCE monolayers likely stems from the same mechanism. Future work should verify their intracellular activity and elucidate their mode of cell entry.

Looking inward to natively produced antimicrobial peptides, many α-defensins neutralize toxins by inducing aggregation and exert broad antibacterial activities (Giesemann et al. 2008; Korbmacher et al. 2020; Fischer et al. 2020; Barthold et al. 2022). Human α-defensin-1 also competitively inhibits glucosyltransferase activity independently of its aggregation mechanism of action (Giesemann et al. 2008). The evolution of these factors with broad antibacterial and anti-virulence activity highlights the importance of targeting both the pathogenic

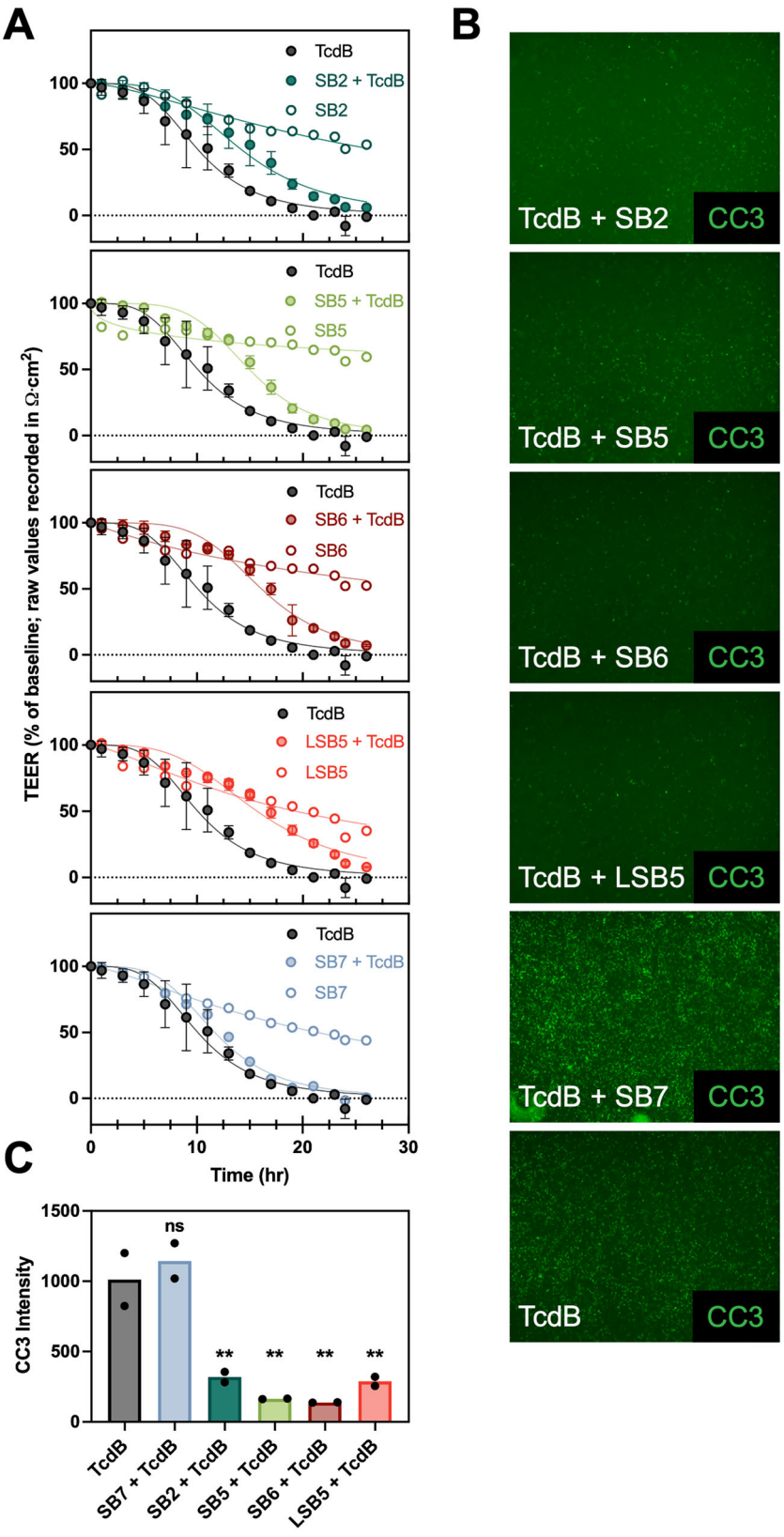

FIGURE 5 | Peptides were evaluated for TcdB neutralization in a human colon epithelial cell (hCE) model. (A) Monolayer TEER measurements for differentiated hCE treated apically and basally with peptide at $t = -1$ h and exposed to TcdB apically and basally at $t = 0$ h. Raw TEER was recorded in units of Ohm cm² (Ω cm²) using the EVOM 2 system, data normalized to baseline. (B) Representative images of immunofluorescence-stained monolayers fixed 26 h posttreatment and (C) cleaved-caspase 3 (CC3) intensity from $n = 2$ images. Images were taken on a BZ-X810 Keyence ×10 objective with BZ-X800 analysis software and processed using FIJI. TcdB was added to DM at 30 pM; peptides were added at 1 mM; TcdB $n = 2$, TcdB + peptide (SB2, SB5, SB6, LSB5) $n = 3$, TcdB + SB7 $n = 1$, peptide (SB2, SB5, SB6, LSB5, SB7) $n = 1$ transwells, TEER means ± SD. One-way ANOVA followed by Dunnett's multiple comparisons test were used. $^{*}p < 0.05$, $^{**}p < 0.01$.

bacteria and their virulence factors. These innate defensins have evolved to wear multiple hats, protecting against many different pathogens, and thus may have killed some potency at the expense of broad activity. Their three-strand β-sheet structure stabilized by three disulfide bonds lends structural and proteolytic stability (Giesemann et al. 2008). Selective maturation of α-defensin-1 for enhanced glucosyltransferase inhibition may provide another promising avenue for developing novel therapeutics for CDI.

Biologics that target virulence factors can complement both conventional antibiotic treatments and emerging live microbial therapies by providing a synergistic route to symptom prevention and management that does not select for antibiotic resistance. In this context, approved biotherapeutics mainly interact with the CROPs and delivery domains, and their mechanism of action reduces cellular entry (Hernandez et al. 2017; Marozsan et al. 2012; Kordus et al. 2022; Murase et al. 2014; Simeon et al. 2021; Yang et al. 2014). Recent efforts have targeted other toxin domains, typically by selecting mAb and nanobody binders that inhibit endosomal translocation, CPD-mediated GTD cleavage, or plasma membrane localization (Liu et al. 2021; Yang et al. 2014; Kroh et al. 2018; Liu et al. 2022). Other drug development efforts reliant on small-molecule inhibitors targeted the enzymatic processes mediated by the GTD and CPD (Heber et al. 2022; Tam et al. 2015; Paparella et al. 2021; Letourneau 2018a, 2018b; Puri et al. 2010). However, to our knowledge, no biologic discovery pipeline has directly targeted the inhibition of key TcdB enzymatic processes. Our study presents the first small biomolecule inhibitor that directly competes with Rho proteins, offering a unique approach to the development of virulence factor-targeted therapies.

Inhibition of Rho protein glucosylation through steric hinderance or displacement is an attractive strategy for preventing the onset of host cellular dysfunction at the final step of the toxins' cycle. However, achieving broad activity is challenging as the same features that differentiate Rho protein preference can disrupt inhibitor binding. Therefore, we targeted a conserved region involved in Rho recognition to minimize toxin escape. However, both this region of the GTD, which undergoes conformational changes upon UDP-glucose binding, and the select peptide inhibitors are inherently flexible, leading to entropic penalties during binding, and thus weaker affinity. At present, the modest affinity of these peptides to the GTD limits their clinical application. To address this issue, next-generation competitive Rho inhibitors could recruit more rigid scaffolds (e.g., cyclic peptides or small protein scaffolds [defensins, DARPins, nanobodies]) or target the more inflexible switch II interface at the α16–17 helices of the GTD. Additionally, it is important to consider the saturation of the GTD with UDP-glucose intracellularly, which affects the orientation of the reactive loop. Further improvements in designing peptide or small protein inhibitors could be gained by targeting the GTD:UDP-glucose complex in lieu of the free GTD. This approach would enable enhanced inhibitor affinity to the most abundant intracellular GTD species and improve the chances of developing broadly active therapeutics. These principles can be directly applied to TcdA, which shares significant homology to TcdB in the reactive loop, but has a distinct Rho binding interface that distinguishes its specificity towards RhoA and other Rho proteins (Genth et al. 2014; Liu 2021; B. Chen et al. 2022). Lastly, future drug discovery efforts shall investigate combining orthogonal inhibitor classes to block multiple steps in the toxins' pathway and minimize the concentration necessary to produce therapeutic effects.

Author Contributions

C.M.C., S.S., C.M.H., C.F., D.D., E.P., S.T.M., C.K.H., N.C., and S.M. designed research; C.M.C., S.S., C.M.H., C.F., K.B., and E.P performed research, C.M.C., S.S., S.T.M., C.K.H., N.C., and S.M. analyzed data, and C.M.C., S.S., S.T.M., C.K.H., N.C., and S.M. wrote the paper.

Acknowledgments

The authors would like to acknowledge other members of the Crook, Menegatti, Hall, and Magness Labs for their helpful suggestions and ideas that shaped and accelerated this study. The authors gratefully acknowledge the National Science Foundation (CBET-1934284, CBET-2347712), the Novo Nordisk Foundation (NNF19SA0035474), the North Carolina Biotechnology Center (2019-FLG-3841), and the National Institutes of Health (R56-AI177728, 5T32GM133366) for financial support. We also thank Ashleigh Paparella and Vern Schramm for providing the plasmids pET28-TcdB1 GTD-6xHis and PD454-6xHis-Rac1, and peer reviewers for their comments that strengthened this study.

Conflicts of Interest

The authors have filed invention disclosures at their respective universities pertaining to the peptides discussed in this study.

Data Availability Statement

The data that support the findings of this study are available from the corresponding author upon reasonable request.

References

Abdeen, S. J., R. J. Swett, and A. L. Feig. 2010. "Peptide Inhibitors Targeting *Clostridium difficile* Toxins A and B." *ACS Chemical Biology* 5: 1097–1103.

Aktories, K., C. Schwan, and T. Jank. 2017. "*Clostridium difficile* Toxin Biology." *Annual Review of Microbiology* 71: 281–307.

Alonso, C. D., C. P. Kelly, K. W. Garey, et al. 2022. "Ultrasensitive and Quantitative Toxin Measurement Correlates With Baseline Severity, Severe Outcomes, and Recurrence Among Hospitalized Patients With *Clostridioides difficile* Infection." *Clinical Infectious Diseases* 74: 2142–2149.

Barthold, L., S. Heber, C. Q. Schmidt, et al. 2022. "Human α-Defensin-6 Neutralizes *Clostridioides difficile* Toxins TcdA and TcdB by Direct Binding." *International Journal of Molecular Sciences* 23: 4509.

Bassères, E., B. T. Endres, N. Montes-Bravo, et al. 2021. "Visualization of Fidaxomicin Association With the Exosporium Layer of *Clostridioides difficile* spores." *Anaerobe* 69: 102352.

Baunwall, S. M. D., M. M. Lee, M. K. Eriksen, et al. 2020. "Faecal Microbiota Transplantation for Recurrent *Clostridioides difficile* infection: An Updated Systematic Review and Meta-Analysis." *eClinicalMedicine* 29: 100642. https://doi.org/10.1016/j.eclinm.2020.100642.

Carter, G. P., A. Chakravorty, T. A. Pham Nguyen, et al. 2015. "Defining the Roles of TcdA and TcdB in Localized Gastrointestinal Disease, Systemic Organ Damage, and the Host Response During *Clostridium difficile* Infections." *mBio* 6: e00551.

Centers for Disease Control and Prevention (U.S.). 2019. "Antibiotic Resistance Threats in the United States, 2019." https://doi.org/10.15620/cdc:82532.

Chandrasekaran, R., and D. B. Lacy. 2017. "The Role of Toxins in *Clostridium difficile* Infection." *FEMS Microbiology Reviews* 41: 723–750.

Chaves-Olarte, E., M. Weidmann, C. Eichel-Streiber, and M. Thelestam. 1997. "Toxins A and B From *Clostridium difficile* Differ With Respect to Enzymatic Potencies, Cellular Substrate Specificities, and Surface Binding to Cultured Cells." *Journal of Clinical Investigation* 100: 1734–1741.

Chen, B., Z. Liu, K. Perry, and R. Jin. 2022. "Structure of the Glucosyltransferase Domain of TcdA in Complex With RhoA Provides Insights Into Substrate Recognition." *Scientific Reports* 12: 9028.

Chen, P., and R. Jin. 2023. "Receptor Binding Mechanisms of *Clostridioides difficile* Toxin B and Implications for Therapeutics Development." *FEBS Journal* 290: 962–969.

Chen, P., K. Lam, Z. Liu, et al. 2019. "Structure of the Full-Length *Clostridium difficile* Toxin B." *Nature Structural & Molecular Biology* 26: 712–719.

Chen, P., J. Zeng, Z. Liu, et al. 2021. "Structural Basis for CSPG4 as a Receptor for TcdB and a Therapeutic Target in *Clostridioides difficile* Infection." *Nature Communications* 12: 3748.

Copeland, R. A. 2023. *Enzymes: A Practical Introduction to Structure, Mechanism, and Data Analysis*. Wiley, 2023.

Day, K., R. Prodromou, S. Saberi Bosari, et al. 2019. "Discovery and Evaluation of Peptide Ligands for Selective Adsorption and Release of Cas9 Nuclease on Solid Substrates." *Bioconjugate Chemistry* 30: 3057–3068.

Dubberke, E. R., C. H. Lee, R. Orenstein, S. Khanna, G. Hecht, and D. N. Gerding. 2018. "Results From a Randomized, Placebo-Controlled Clinical Trial of a RBX2660-A Microbiota-Based Drug for the Prevention of Recurrent *Clostridium difficile* Infection." *Clinical Infectious Diseases* 67: 1198–1204.

Durmusoglu, D., C. M. Catella, E. F. Purnell, S. Menegatti, and N. C. Crook. 2021. "Design and In Situ Biosynthesis of Precision Therapies Against Gastrointestinal Pathogens." *Current Opinion in Physiology* 23: 100453.

D'Urzo, N., E. Malito, M. Biancucci, et al. 2012. "The Structure of *Clostridium difficile* Toxin A Glucosyltransferase Domain Bound to Mn2+ and UDP Provides Insights into Glucosyltransferase Activity and Product Release." *FEBS Journal* 279: 3085–3097.

Fischer, S., A. K. Ückert, M. Landenberger, et al. 2020. "Human Peptide α-defensin-1 Interferes With *Clostridioides difficile* Toxins TcdA, TcdB, and CDT." *FASEB Journal* 34: 6244–6261.

Genisyuerek, S., P. Papatheodorou, G. Guttenberg, R. Schubert, R. Benz, and K. Aktories. 2011. "Structural Determinants for Membrane Insertion, Pore Formation and Translocation of *Clostridium difficile* Toxin B." *Molecular Microbiology* 79: 1643–1654.

Genth, H., S. Pauillac, I. Schelle, et al. 2014. "Haemorrhagic Toxin and Lethal Toxin From *Clostridium sordellii* Strain vpi9048: Molecular Characterization and Comparative Analysis of Substrate Specificity of the Large Clostridial Glucosylating Toxins." *Cellular Microbiology* 16: 1706–1721.

Gerhard, R., E. Frenzel, S. Goy, and A. Olling. 2013. "Cellular Uptake of *Clostridium difficile* TcdA and Truncated TcdA Lacking the Receptor Binding Domain." *Journal of Medical Microbiology* 62: 1414–1422.

Giesemann, T., G. Guttenberg, and K. Aktories. 2008. "Human α-Defensins Inhibit *Clostridium difficile* Toxin B." *Gastroenterology* 134: 2049–2058.

Heber, S., L. Barthold, J. Baier, et al. 2022. "Inhibition of *Clostridioides difficile* Toxins TcdA and TcdB by Ambroxol." *Frontiers in Pharmacology* 12: 809595.

Hernandez, L. D., H. K. Kroh, E. Hsieh, et al. 2017. "Epitopes and Mechanism of Action of the *Clostridium difficile* Toxin A-Neutralizing Antibody Actoxumab." *Journal of Molecular Biology* 429: 1030–1044.

Hernandez, L. D., F. Racine, L. Xiao, et al. 2015. "Broad Coverage of Genetically Diverse Strains of *Clostridium difficile* by Actoxumab and Bezlotoxumab Predicted by In Vitro Neutralization and Epitope Modeling." *Antimicrobial Agents and Chemotherapy* 59: 1052–1060.

Ho, J. G. S., A. Greco, M. Rupnik, and K. K.-S. Ng. 2005. "Crystal Structure of Receptor-Binding C-Terminal Repeats From *Clostridium difficile* Toxin A." *Proceedings of the National Academy of Sciences* 102: 18373–18378.

Honorato, R. V., M. E. Trellet, B. Jiménez-García, et al. 2024. "The HADDOCK2.4 Web Server for Integrative Modeling of Biomolecular Complexes." *Nature Protocols* 19: 3219–3241. https://www.nature.com/articles/s41596-024-01011-0.

Jank, T., T. Giesemann, and K. Aktories. 2007. "*Clostridium difficile* Glucosyltransferase Toxin B-Essential Amino Acids for Substrate Binding." *Journal of Biological Chemistry* 282: 35222–35231.

Jank, T., M. O. P. Ziegler, G. E. Schulz, and K. Aktories. 2008. "Inhibition of the Glucosyltransferase Activity of Clostridial Rho/Ras-Glucosylating Toxins by Castanospermine." *FEBS Letters* 582: 2277–2282.

Johnson, S. 2009. "Recurrent *Clostridium difficile* Infection: A Review of Risk Factors, Treatments, and Outcomes." *Journal of Infection* 58: 403–410.

Johnson, S., V. Lavergne, A. M. Skinner, et al. 2021. "Clinical Practice Guideline by the Infectious Diseases Society of America (IDSA) and Society for Healthcare Epidemiology of America (SHEA): 2021 Focused Update Guidelines on Management of *Clostridioides difficile* Infection in Adults." *Clinical Infectious Diseases* 73: e1029–e1044.

Just, I., M. Wilm, J. Selzer, et al. 1995. "The Enterotoxin From *Clostridium difficile* (ToxA) Monoglucosylates the Rho Proteins." *Journal of Biological Chemistry* 270: 13932–13936.

Just, I., J. Selzer, M. Wilm, C. von Eichel-Streiber, M. Mann, and K. Aktories. 1995. "Glucosylation of Rho Proteins by *Clostridium difficile* Toxin B." *Nature* 375: 500–503.

Khoruts, A., C. Staley, and M. J. Sadowsky. 2021. "Faecal Microbiota Transplantation for *Clostridioides difficile*: Mechanisms and Pharmacology." *Nature Reviews Gastroenterology & Hepatology* 18: 67–80.

Kilgore, R., W. Chu, D. Bhandari, et al. 2023. "Development of Peptide Affinity Ligands for the Purification of Polyclonal and Monoclonal Fabs From Recombinant Fluids." *Journal of Chromatography A* 1687: 463701.

Korbmacher, M., S. Fischer, M. Landenberger, P. Papatheodorou, K. Aktories, and H. Barth. 2020. "Human α-Defensin-5 Efficiently Neutralizes *Clostridioides difficile* Toxins TcdA, TcdB, and CDT." *Frontiers in Pharmacology* 11. https://www.frontiersin.org/journals/pharmacology/articles/10.3389/fphar.2020.01204/full.

Kordus, S. L., A. K. Thomas, and D. B. Lacy. 2022. "*Clostridioides difficile* Toxins: Mechanisms of Action and Antitoxin Therapeutics." *Nature Reviews Microbiology* 20: 285–298.

Kroh, H. K., R. Chandrasekaran, Z. Zhang, et al. 2018. "A Neutralizing Antibody That Blocks Delivery of the Enzymatic Cargo of *Clostridium difficile* toxin TcdB into Host Cells." *Journal of Biological Chemistry* 293: 941–952.

Letourneau, J. J., I. L. Stroke, D. W. Hilbert, et al. 2018a. "Identification and Initial Optimization of Inhibitors of *Clostridium difficile* (*C. difficile*) Toxin B (TcdB)." *Bioorganic & Medicinal Chemistry Letters* 28: 756–761.

Letourneau, J. J., I. L. Stroke, D. W. Hilbert, et al. 2018b. "Synthesis and SAR Studies of Novel Benzodiazepinedione-Based Inhibitors of *Clostridium difficile* (*C. difficile*) toxin B (TcdB)." *Bioorganic & Medicinal Chemistry Letters* 28: 3601–3605.

Liu, J., M. Kothe, J. Zhang, et al. 2022. "Novel Structural Insights for a Pair of Monoclonal Antibodies Recognizing Non-Overlapping Epitopes of the Glucosyltransferase Domain of *Clostridium difficile* Toxin B." *Current Research in Structural Biology* 4: 96–105.

Liu, Z., S. Zhang, P. Chen, et al. 2021. "Structural Basis for Selective Modification of Rho and Ras GTPases by *Clostridioides difficile* Toxin B." *Science Advances* 7: eabi4582.

Loughney, J. W., C. Lancaster, C. E. Price, V. M. Hoang, S. Ha, and R. R. Rustandi. 2017. "Development of a Non-Radiolabeled Glucosyltransferase Activity Assay for *C. difficile* Toxin A and B Using Ultra Performance Liquid Chromatography." *Journal of Chromatography A* 1498: 169–175.

Lyras, D., J. R. O'Connor, P. M. Howarth, et al. 2009. "Toxin B Is Essential for Virulence of *Clostridium difficile*." *Nature* 458: 1176–1179.

Manse, J. S., and M. R. Baldwin. 2015. "Binding and Entry of *Clostridium difficile* Toxin B Is Mediated by Multiple Domains." *FEBS Letters* 589: 3945–3951.

Mansfield, M. J., B. J. M. Tremblay, J. Zeng, et al. 2020. "Phylogenomics of 8,839 *Clostridioides difficile* Genomes Reveals Recombination-Driven Evolution and Diversification of Toxin A and B." *PLoS Pathogens* 16: e1009181.

Marozsan, A. J., D. Ma, K. A. Nagashima, et al. 2012. "Protection Against *Clostridium difficile* Infection With Broadly Neutralizing Antitoxin Monoclonal Antibodies." *Journal of Infectious Diseases* 206: 706–713.

McGovern, B. H., C. B. Ford, M. R. Henn, et al. 2021. "SER-109, an Investigational Microbiome Drug to Reduce Recurrence After *Clostridioides difficile* Infection: Lessons Learned From a Phase 2 Trial." *Clinical Infectious Diseases* 72: 2132–2140.

Murase, T., L. Eugenio, M. Schorr, et al. 2014. "Structural Basis for Antibody Recognition in the Receptor-Binding Domains of Toxins A and B From *Clostridium difficile*." *Journal of Biological Chemistry* 289: 2331–2343.

Normington, C., I. B. Moura, J. A. Bryant, et al. 2021. "Biofilms Harbour *Clostridioides difficile*, serving as a Reservoir for Recurrent Infection." *NPJ Biofilms and Microbiomes* 7: 16.

Ok, M. T., J. Liu, R. J. Bliton, et al. 2023. "A Leaky Human Colon Model Reveals Uncoupled Apical/Basal Cytotoxicity in Early *Clostridioides difficile* Toxin Exposure." *American Journal of Physiology-Gastrointestinal and Liver Physiology* 324: G262–G280.

Paparella, A. S., B. L. Aboulache, R. K. Harijan, K. S. Potts, P. C. Tyler, and V. L. Schramm. 2021. "Inhibition of *Clostridium difficile* TcdA and TcdB Toxins With Transition State Analogues." *Nature Communications* 12: 6285.

Paparella, A. S., S. M. Cahill, B. L. Aboulache, and V. L. Schramm. 2022. "*Clostridioides difficile* TcdB Toxin Glucosylates Rho GTPase by an S_Ni Mechanism and Ion Pair Transition State." *ACS Chemical Biology* 17: 2507–2518.

Pruitt, R. N., N. M. Chumbler, S. A. Rutherford, et al. 2012. "Structural Determinants of *Clostridium difficile* Toxin A Glucosyltransferase Activity." *Journal of Biological Chemistry* 287: 8013–8020.

Puri, A. W., P. J. Lupardus, E. Deu, et al. 2010. "Rational Design of Inhibitors and Activity-Based Probes Targeting *Clostridium difficile* Virulence Factor TcdB." *Chemistry & Biology* 17: 1201–1211.

Raeisi, H., M. Azimirad, A. Nabavi-Rad, H. Asadzadeh Aghdaei, A. Yadegar, and M. R. Zali. 2022. "Application of Recombinant Antibodies for Treatment of *Clostridioides difficile* Infection: Current Status and Future Perspective." *Frontiers in immunology* 13: 972930.

Reinert, D. J., T. Jank, K. Aktories, and G. E. Schulz. 2005. "Structural Basis for the Function of *Clostridium difficile* Toxin B." *Journal of Molecular Biology* 351: 973–981.

Rupnik, M., M. H. Wilcox, and D. N. Gerding. 2009. "*Clostridium difficile* Infection: New Developments in Epidemiology and Pathogenesis." *Nature Reviews Microbiology* 7: 526–536.

Saberi-Bosari, S., M. Omary, A. Lavoie, et al. 2019. "Affordable Microfluidic Bead-Sorting Platform for Automated Selection of Porous Particles Functionalized With Bioactive Compounds." *Scientific Reports* 9: 7210.

Sarma, S., C. M. Catella, E. T. San Pedro, et al. 2023. "Design of 8-mer Peptides That Block *Clostridioides difficile* Toxin A in Intestinal Cells." *Communications Biology* 6: 878.

Schäffler, H., and A. Breitrück. 2018. "*Clostridium difficile* – From Colonization to Infection." *Frontiers in Microbiology* 9: 646.

Segel, I. H.1935 [1975]. *Enzyme Kinetics: Behavior and Analysis of Rapid Equilibrium and Steady State Enzyme Systems*. Wiley.

Shen, A., P. J. Lupardus, M. M. Gersch, et al. 2011. "Defining an Allosteric Circuit in the Cysteine Protease Domain of *Clostridium difficile* toxins." *Nature Structural & Molecular Biology* 18: 364–371.

Shen, E., K. Zhu, D. Li, et al. 2020. "Subtyping Analysis Reveals New Variants and Accelerated Evolution of *Clostridioides difficile* toxin B." *Communications Biology* 3: 347.

Simeon, R. A., Y. Zeng, V. Chonira, et al. 2021. "Protease-Stable Darpins as Promising Oral Therapeutics." *Protein Engineering Design and Selection* 34: gzab028. https://doi.org/10.1093/protein/gzab028.

Song, L., M. Zhao, D. C. Duffy, et al. 2015. "Development and Validation of Digital Enzyme-Linked Immunosorbent Assays for Ultrasensitive Detection and Quantification of *Clostridium difficile* Toxins in Stool." *Journal of Clinical Microbiology* 53: 3204–3212.

Spigaglia, P. 2016. "Recent Advances in the Understanding of Antibiotic Resistance in *Clostridium difficile* Infection." *Therapeutic Advances in Infectious Disease* 3: 23–42.

Stewart, D., F. Anwar, and G. Vedantam. 2020. "Anti-Virulence Strategies for *Clostridioides difficile* Infection: Advances and Roadblocks." *Gut Microbes* 12: 1802865.

Tam, J., G. L. Beilhartz, A. Auger, P. Gupta, A. G. Therien, and R. A. Melnyk. 2015. "Small Molecule Inhibitors of *Clostridium difficile* Toxin B-Induced Cellular Damage." *Chemistry & Biology* 22: 175–185.

Tao, L., J. Zhang, P. Meraner, et al. 2016. "Frizzled Proteins Are Colonic Epithelial Receptors for *C. difficile* toxin B." *Nature* 538: 350–355.

Theriot, C. M., A. A. Bowman, and V. B. Young. 2016. "Antibiotic-Induced Alterations of the Gut Microbiota Alter Secondary Bile Acid Production and Allow for *Clostridium difficile* Spore Germination and Outgrowth in the Large Intestine." *mSphere* 1: e00045-15.

Villafuerte Gálvez, J. A., and C. P. Kelly. 2017. "Bezlotoxumab: Anti-Toxin B Monoclonal Antibody to Prevent Recurrence of *Clostridium difficile* Infection." *Expert Review of Gastroenterology & Hepatology* 11: 611–622.

Xiao, X., Z. Kuang, J. M. Slocik, et al. 2018. "Advancing Peptide-Based Biorecognition Elements for Biosensors Using In-Silico Evolution." *ACS Sensors* 3: 1024–1031.

Xiao, X., S. Sarma, S. Menegatti, N. Crook, S. T. Magness, and C. K. Hall. 2022. "*In Silico* Identification and Experimental Validation of Peptide-Based Inhibitors Targeting *Clostridium difficile* Toxin A." *ACS Chemical Biology* 17: 118–128.

Xiao, X., B. Zhao, P. F. Agris, and C. K. Hall. 2016. "Simulation Study of the Ability of a Computationally-Designed Peptide to Recognize Target tRNALys3 and Other Decoy tRNAs." *Protein Science* 25: 2243–2255.

Yadegar, A., H. Bar-Yoseph, T. M. Monaghan, et al. 2024. "Fecal Microbiota Transplantation: Current Challenges and Future Landscapes." *Clinical Microbiology Reviews* 37: e0006022.

Yang, Z., D. Schmidt, W. Liu, et al. 2014. "A Novel Multivalent, Single-Domain Antibody Targeting TcdA and TcdB Prevents Fulminant *Clostridium difficile* Infection in Mice." *Journal of Infectious Diseases* 210: 964–972.

Yuan, P., H. Zhang, C. Cai, et al. 2015. "Chondroitin Sulfate Proteoglycan 4 Functions as the Cellular Receptor for *Clostridium difficile* Toxin B." *Cell Research* 25: 157–168.

van Zundert, G. C. P., J. P. G. L. M. Rodrigues, M. Trellet, et al. 2016. "The HADDOCK2.2 Web Server: User-Friendly Integrative Modeling of Biomolecular Complexes." *Journal of Molecular Biology* 428: 720–725.

Supporting Information

Additional supporting information can be found online in the Supporting Information section.
cmc185-pet28-w-tcdb2-gtd. cmc186-pet28-w-tcdb3-gtd. cmc211-pet28-w-tcdb1-gtd-6xhis-paparella-et-al-fixed. TcdB Peptide Supplementary HDX. TcdB Peptides Methods 03Oct25. **Figure S1.** TcdB1 inhibitor screen. Glucosyltransferase activity was measured using 10 nM TcdB1 GTD, 1 mM inhibitor, 5 μM Rac1, and varied UDP-glucose concentrations. Inhibitor data were fit to the mixed inhibition mode equation. Data represent n = 2 replicates. **Figure S2.** TcdB2 inhibitor screen. Glucosyltransferase activity was measured using 10 nM TcdB2 GTD, 1 mM inhibitor, 5 μM Rac1, and varied UDP-glucose concentrations. Inhibitor data were fit to the mixed inhibition mode equation. Data represent n = 2 replicates. **Figure S3.** TcdB3 inhibitor screen. Glucosyltransferase activity was measured using 10 nM TcdB3 GTD, 1 mM inhibitor, 5 μM Rac1, and varied UDP-glucose concentrations. Inhibitor data were fit to the mixed inhibition mode equation. Data represent n = 2 replicates. **Figure S4.** Peptides SB2, SB5, and SB6 act as non-competitive inhibitors with respect to UDP-glucose. **Figure S5.** Peptides SB2, SB5, and SB6 act as competitive inhibitors with respect to Rac1. **Figure S6.** TcdB1, TcdB2, and TcdB3 GTD inhibition by castanospermine. **Figure S7.** HDX epitope mapping: deuterium exchange rates for mapped peptides. **Figure S8.** Representative conformations and binding free energies of SB5 and scrambled SB5 (ScSB5) to various regions of TcdB. **Figure S9.** Effect of peptides on transepithelial electrical resistance (TEER) in human colonic epithelial monolayers. **Table S1.** Solid phase peptide library screening sequences. **Table S2.** Amino acid constraints used for in-silico optimization cases. **Table S3.** Deconvolution of inhibition mechanism by titrating single substrates in a bi-reactant glucosyltransferase reaction. **Table S4.** HDX-MS epitope mapping peptide summary.